Combined SANS–SAXS Study of Blends of Styrene–Butadiene Block Copolymer with Deuteriated Polybutadiene

Shuichi Nojima

Department of Applied Chemistry, Nagoya University, Nagoya, Japan

Ryong-Joon Roe* and David Rigby

Department of Materials Science and Engineering, University of Cincinnati, Cincinnati, Ohio 45221-0012

C. C. Han

National Institute of Standards and Technology, Washington, D.C. 20234

Received December 14, 1989; Revised Manuscript Received March 5, 1990

ABSTRACT: The structure of the blends containing styrene–butadiene diblock copolymer (M_n = 21 000, styrene content 76.6% by weight) and deuteriated polybutadiene (M_n = 1980) has been studied by the combination of small-angle neutron and X-ray scattering techniques. Blends containing 3, 10, 20, 30, 40, and 50 wt % of the block copolymer were studied at temperatures spanning from room temperature to about 200 °C. The small-angle neutron scattering arises as a result of the contrast in the scattering length density between the deuteriated polybutadiene and the hydrogenated block copolymer, while the small-angle X-ray scattering arises as a result of the electron density contrast between the styrene and butadiene components. The structural information obtained by these techniques includes the mean distance between micelles (or microdomains), the thickness of the interfacial region, and the specific interfacial area. With blends of copolymer concentrations (3 and 10%) the effective radius of the micelle core, $\langle R \rangle$, and the hard-sphere radius, $\langle R_{HS} \rangle$ (i.e., the radius of the nearest approach of neighboring micelles), were also determined.

Introduction

In this work we have utilized both the small-angle neutron scattering (SANS) and small-angle X-ray scattering (SAXS) techniques in combination to study the structure of the mixture of styrene–butadiene diblock copolymer and deuteriated polybutadiene as a function of temperature and composition. The principles governing the structure of pure block copolymers, both as a function of the composition (relative lengths of the blocks) and as a function of temperature (including the phenomenon of the onset of microphase separation), are now fairly well understood as a result of extensive studies, both theoretical[1] and experimental,[2] in recent years. When a block copolymer AB is mixed with a homopolymer A, an added complexity in the structure and behavior of the mixtures arises,[3] especially as a result of the interaction of the macroscopic phase separation of the two-component system with the microphase separation of the block copolymer itself. The phase diagrams of such mixtures have thus been shown[4] to be unusually rich in features that are yet to be explored in detail. In our continuing effort to understand the behavior of homopolymer–block copolymer mixtures, we earlier studied the solubility[4,5] of polystyrene added to the styrene–butadiene block copolymer, the structure of micelles[6,7] formed when a small amount of block copolymer is added to low molecular weight polybutadiene, and the effect of added polystyrene[8] of various molecular weights on the microphase-separation transition of block copolymer. In the present work the mixtures studied contain 3, 10, 20, 30, 40, and 50 wt % of styrene–butadiene copolymer (M_n = 21 000, styrene content 76.6% by weight) in deuteriated polybutadiene (M_n = 1980), and the small-angle scattering data were obtained at temperatures spanning from room temperature to about 200 °C.

The principles of coherent small-angle scattering of neutrons and of X-rays from polymer blends are the same, except for differences in the contrast factors that give rise to the scattering between the two cases. In our present system of study, there are potentially three regions of different densities, the styrene block of the copolymer, the hydrogenated butadiene block of the copolymer, and the deuteriated polybutadiene. The coherent neutron scattering length densities and electron densities of these three regions, calculated for 80 °C, are listed in Table I. The data here indicate that the neutron scattering will occur mainly because of the contrast between the block copolymer and the deuteriated polybutadiene, while the X-ray scattering will occur mainly because of the contrast between polystyrene and polybutadiene. Thus, the combination of these two techniques can potentially provide information about the three regions separately.

Table I
Contrast Factors at 80 °C

	neutron scattering length density, cm/nm^3	electron density, e/nm^3
polystyrene	13.93×10^{-12}	335.2
polybutadiene	3.93	283.1
deuteriated polybutadiene	63.91	287.8

Experimental Section

Materials. The styrene–butadiene block copolymer has a styrene content of 76.6% by weight, M_n = 21 000, M_w/M_n = 1.05, and the microstructure of its butadiene block is 48% trans-1,4 and 24% cis-1,4. This is the material designated 75/25 in our previous work[7] and was kindly supplied by Dr. H. L. Hsieh of Phillips Petroleum Co. The deuteriated polybutadiene was synthesized in our laboratory with the monomer purchased from Cambridge Isotope Laboratories.[9] The anionic polymerization was carried out under vacuum with *n*-butyllithium as initiator. The monomer/initiator ratio was adjusted to obtain a deuteriated polybutadiene that closely matched the molecular weight of the (hydrogenated) polybutadiene used in our earlier work.[7] Its M_n, determined by vapor phase osmometry, is 1980, and its M_w/M_n ratio, determined by GPC, is 1.08.

0024-9297/90/2223-4305$02.50/0

SAXS and SANS Measurements. The small-angle X-ray scattering measurement was performed with a Kratky camera fitted with a M. Braun linear position-sensitive detector. Ni-filtered Cu Kα radiation from a Philips XRG 3100 generator operating at 45 kV and 35 mA was used. Correction for the slit-length smearing was applied by means of Strobl's algorithm.[10] The small-angle neutron scattering measurement was performed at the Research Reactor of the National Institute of Standards and Technology. The instrument has been described elsewhere.[11] In this study, a two-aperture configuration of 27 and 12 mm was used for collimation. A velocity selector was used to monochromatize neutrons at wavelength λ equal to 6 and 9 Å for two different scheduled occasions of measurement. The wavelength distribution, $\Delta\lambda/\lambda$, was ca. 0.2. Samples containing 10, 20, and 40% copolymer were studied with neutron beams of λ = 9 Å while the others were studied with λ = 6 Å. The scattered neutrons were detected by a two-dimensional position-sensitive detector. The final isotropic scattering structure factor was obtained by subtraction of the scattering arising from the empty cell, by correction for the sample transmittance and thickness, and by rescaling to the absolute intensity unit with the use of a secondary dry-silica standard sample, which was calibrated to the absolute scattering intensity of vanadium as described previously.[11] The two-dimensional intensity data were then reduced to one-dimensional data through a circular average. A copper heating block with PID control was used to control the specimen temperature to within 0.5 °C of desired temperature during measurement.

The following specific volume values were used to calculate the electron density and neutron scattering length density at various temperatures

$$V_{sp}(\text{PS}) = 0.9217 + 5.412 \times 10^{-4}T + 1.687 \times 10^{-7}T^2$$

$$V_{sp}(\text{h-PB}) = 1.1138 + 8.24 \times 10^{-4}T$$

$$V_{sp}(\text{d-PB}) = 0.9870 + 7.30 \times 10^{-4}T$$

where T denotes the temperature in degrees centigrade. The specific volume of polystyrene was taken from data given by Richardson and Savill.[12] The specific volume of hydrogenated polybutadiene is based on the observed specific volume[7] at 30 °C and the temperature coefficient from the literature.[13] The specific volume of deuteriated polybutadiene is based on the observed specific volume[14] at 23 °C and the assumption that the thermal expansion coefficient, $d \ln V/dT$, for the deuteriated species is the same as that for the hydrogenated species.

Results

(i) Intensity Curves. Figure 1 shows the intensities of X-rays scattered from the blend containing 3% (by volume) block copolymer at several temperatures, and Figure 2 shows the intensities of neutrons scattered from the blend containing 40% (by volume) copolymer. Plotted in Figure 1 are the "intensities", which are equal to $I(s)/(\Delta\rho_{SB})^2$, where $I(s)$ is the observed (slit-desmeared) X-ray intensities per unit volume in absolute units (e^2/nm^3), and $\Delta\rho_{SB}$ is the electron density difference between polystyrene and polybutadiene at the respective temperatures. Similarly, in the plots in Figure 2, the observed neutron scattering intensities $I(s)$, obtained in absolute units per unit volume, were divided by $(\Delta b_{HD})^2$, where Δb_{HD} is the difference between the neutron scattering length density of deuteriated polybutadiene and the weighted-average scattering length density of the block copolymer. The "intensity" values in these two figures therefore are in units of nanometers cubed and are directly comparable to each other.

The X-ray and neutron scattering curves are very similar to each other when data obtained at the same temperature and composition are compared. At all compositions, the intensity of scattering, in general, decreases with increasing temperature. At the lowest concentration of the copolymer studied, i.e., ϕ = 0.03, the intensity decreases monotonically

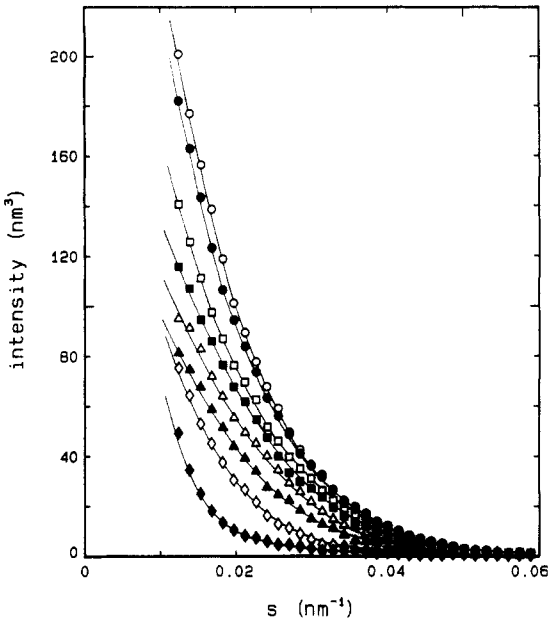

Figure 1. X-ray intensities scattered from a mixture containing 3% block copolymer in deuteriated polybutadiene, measured at 39.3, 80.1, 100.2, 110.5, 120.1, 130.0, 140.8, and 150.4 °C (in the order of decreasing intensity). The scattering angle is expressed in s (=2 sin θ/λ), and the intensity value shown gives the observed (slit-desmeared) intensity in absolute units (e^2/nm^3), after division by $(\Delta\rho_{SB})^2$, where $\Delta\rho_{SB}$ is the electron density difference (e/nm^3) between polystyrene and polybutadiene at the respective temperatures.

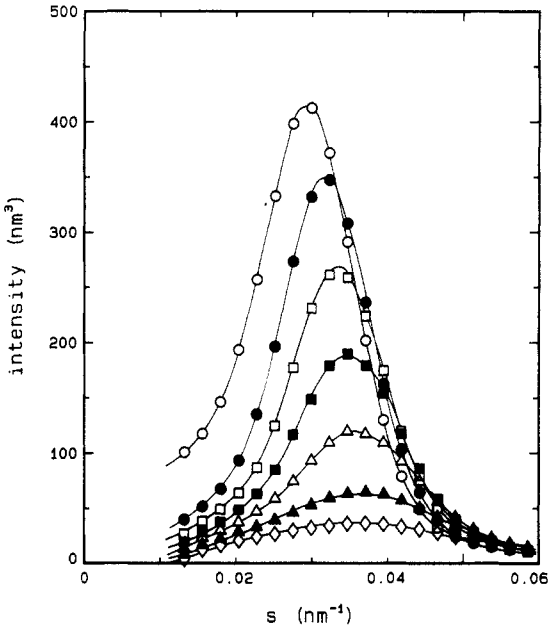

Figure 2. Neutron intensities scattered from a mixture containing 40% block copolymer in deuteriated polybutadiene, measured at 40.0, 98.8, 118.8, 137.9, 158.6, 179.7, and 199.7 °C (in the order of decreasing intensity). The intensity value shown is the observed neutron scattering intensity in absolute units, which was then divided by $(\Delta b_{HD})^2$, where Δb_{HD} is the difference between the neutron scattering length density of deuteriated polybutadiene and the weighted-average scattering length density of the block copolymer at the respective temperatures.

with increasing scattering angle s (=2 sin θ/λ), as seen in Figure 1. With blends containing higher amounts of copolymer, the intensity curves show a maximum, and the angular position, s_{max}, of the intensity maximum is higher with higher copolymer concentration and at higher temperature (at least at temperatures above 80 °C). The value of $d = 1/s_{max}$, a measure of the size scale of the

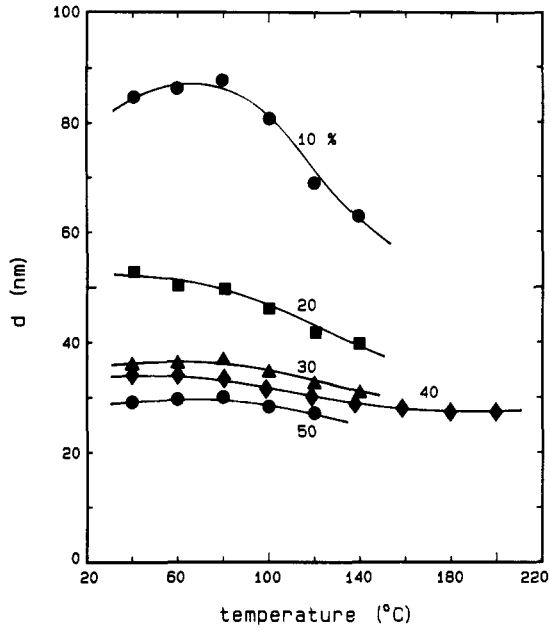

Figure 3. From the observed neutron intensity curves (cf. Figure 2), the angle, s_{max}, of intensity maximum evaluated, and its reciprocal $d = 1/s_{max}$ plotted against temperature. The volume fraction of block copolymer in the sample is indicated in the plot.

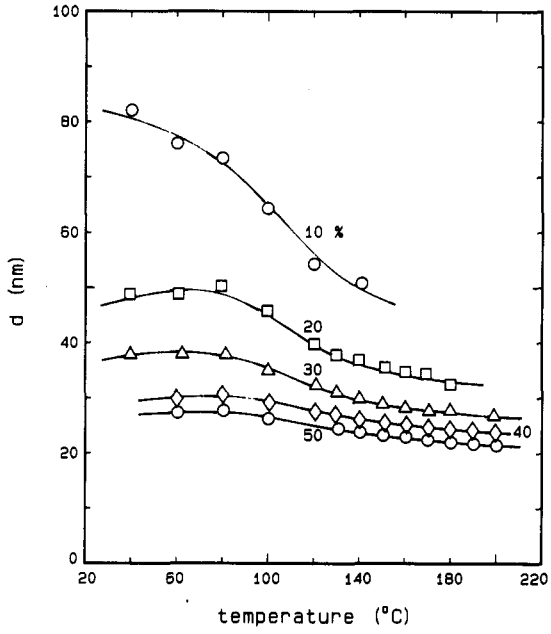

Figure 4. Similar to Figure 3 but the results here derived from the observed X-ray intensity curves.

structure present in the blends, has been evaluated from all the measured scattering curves and is plotted in Figures 3 and 4. The degree of agreement between the d values obtained by neutron and by X-ray is fair and gives some indication of the degree of accuracy of the intensity curves themselves. The data for 60 and 140 °C in Figures 3 and 4 are replotted in Figure 5 to show the variation in d with composition of the blends more clearly. At the low concentration of copolymer, where the copolymer is expected to be present as individual spherical micelles, the d values probably indicate the average separation distance between micelles. As more copolymer is added, the mean separation distance between the copolymer micelles (or microdomains) is observed to decrease. If the size of the micelles (or microdomains) does not change much with composition, d may vary as ϕ^{-a} with $a = {}^1/_3$. The data points in the log–log plot of Figure 5 lie roughly on a

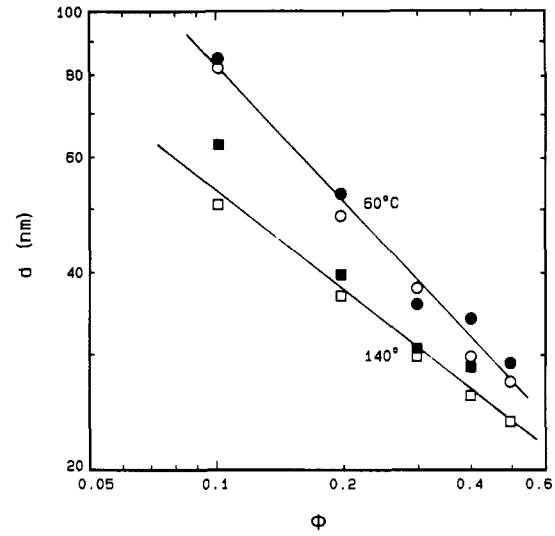

Figure 5. d values shown in Figures 3 and 4 replotted in log–log plot against the volume fraction, ϕ, of the copolymer in the samples. The filled symbols refer to results obtained from the neutron data and the open symbols from the X-ray data.

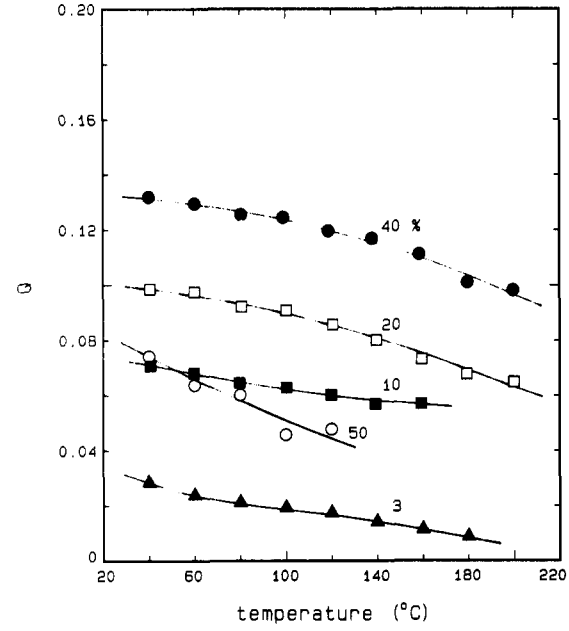

Figure 6. Invariant Q, evaluated from the observed neutron intensities in accordance with eq 1, plotted against temperature. The volume fraction, ϕ, of copolymer contained in the sample is indicated in the plot.

straight line, but the exponent a is equal to about 0.68 at 60 °C and 0.48 at 140 °C. This suggests either that the mean dimension of the microdomains is becoming smaller as ϕ increases or that the spherical micelles present at low ϕ are gradually transformed into cylindrical or lamellar shape with increasing ϕ.

(ii) Invariant Q. Both the neutron and X-ray scattering intensities increase with increasing amount of copolymer and decrease with increasing temperature. These trends can be seen directly from the scattering curves but can be quantified by means of the invariant Q defined by

$$Q = 4\pi \int s^2 I(s)\, ds \qquad (1)$$

Figures 6 and 7 show the Q values evaluated from the neutron and X-ray scattering intensities. In performing the integration indicated by eq 1, the intensity at high scattering angles (for $s > 0.10$ nm^{-1} in the case of SAXS and for $s > 0.12$–0.15 nm^{-1} in the case of SANS) was

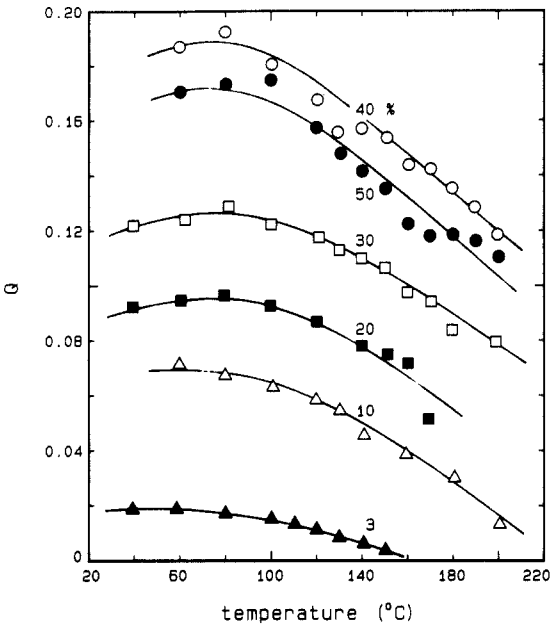

Figure 7. Invariant Q, evaluated from the observed X-ray intensities, plotted against temperature.

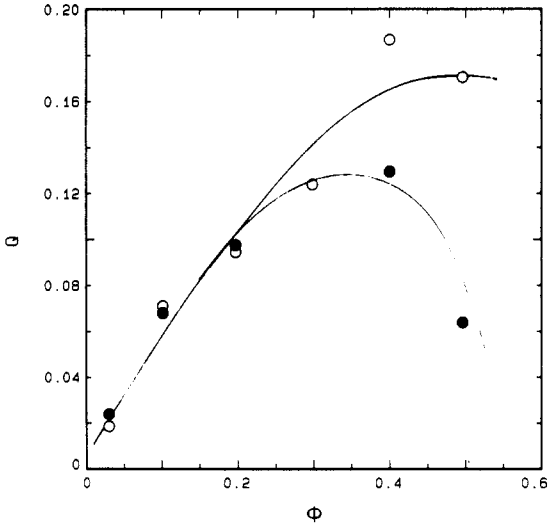

Figure 8. Invariant Q, determined at 60 °C, plotted against the volume fraction, ϕ, of copolymer in the mixture. The solid symbols refer to results obtained from neutron scattering data and the open symbols from X-ray data.

approximated by Porod's law extrapolation. As in Figures 1 and 2, the intensities were normalized with respect to their contrast factors; that is, the observed intensities in absolute units were divided by either $(\Delta b_{HD})^2$ or $(\Delta \rho_{SB})^2$ before the integration indicated by eq 1 was performed, so that the Q values in Figures 6 and 7 are directly comparable to each other. The invariant Q gives the mean-square fluctuation of density (electron density or neutron scattering length density) in the sample. With a two-phase system, that is, a sample containing regions of only two different densities, the value of Q (evaluated with the intensity normalized in the manner described above) is equal to $f(1-f)$, where f is the volume fraction of the regions of one of the two densities. The differences in the data between Figures 6 and 7 reflect the different ways in which the sample volume is divided into regions of high and low densities, depending on whether electron density or neutron scattering length density is involved. The 60 °C data are replotted in Figure 8 against the copolymer volume fraction, ϕ, and it shows that at low ϕ the values of Q from neutron and X-ray data are comparable, but at high ϕ the Q values from neutron data are much lower than the values from X-ray data. Such a drop in the Q values from neutron data at high volume concentrations of copolymer is consistent with the fact that the corona (or the butadiene blocks of the copolymer) is highly swollen with the deuteriated polybutadiene, as will be discussed more fully in the Discussion.

(iii) Porod's Law Analysis. The neutron scattering intensity data at high angles were analyzed in accordance with Porod's law to evaluate the specific interfacial area,[15] S/V, and the thickness parameter,[16] σ, of the interfacial layer. Because of the large contrast in the scattering length densities between the deuteriated and hydrogenated species in the system (and the very small contrast between the hydrogenated polystyrene and polybutadiene), as shown in Table I, our sample can be regarded, to a good approximation, to possess a two-phase structure in interpreting the neutron scattering data. Thus, the intensity in Porod's region can be fitted[17] by

$$I(s) = (1/8\pi^3)(a_1 - a_2)^2(S/V)s^{-4}\exp(-4\pi^2\sigma^2 s^2) + I_b \quad (2)$$

where $I(s)$ is the scattered intensity in absolute units per unit volume of the sample a_1 and a_2 are the scattering length densities of phase 1 and phase 2, respectively, S/V is the interfacial area per unit volume, σ is the parameter that is proportional to the interfacial layer thickness, and I_b is the background intensity (including incoherent scattering). The scattering length density contrast can be written as

$$a_1 - a_2 = (\eta_1 - \eta_2)(a_H - a_D) \quad (3)$$

where η_1 and η_2 are the volume fractions of protonated species (block copolymer) in phase 1 and phase 2, respectively, and a_H and a_D are the scattering length densities of the block copolymer and of the deuteriated polybutadiene, respectively. The concentration of dissolved block copolymer in the deuteriated polybutadiene matrix is small (except above 150 °C), and therefore setting $\eta_2 = 0$ (and letting $\eta \equiv \eta_1$), we have

$$a_1 - a_2 = \eta(a_H - a_D) \quad (4)$$

Thus, instead of eq 2 we have

$$I(s)/(\Delta a)^2 = (1/8\pi^3)(\eta^2 S/V)s^{-4}\exp(-4\pi^2\sigma^2 s^2) + I_b \quad (5)$$

where $\Delta a = a_H - a_D$. Equation 5 shows that Porod's law analysis of $I(s)/(\Delta a)^2$ will allow us to evaluate $\eta^2 S/V$ and σ. The effective thickness, t, of the interfacial layer is related to σ by

$$t = (4\sqrt{3}/\pi)\sigma \quad (6)$$

provided the composition profile across the interface conforms[17] to

$$\rho(x) = \frac{\rho_1 + \rho_2}{2} + \frac{\rho_1 - \rho_2}{2}\tanh(2x/t) \quad (7)$$

which is predicted theoretically for interfaces between amorphous polymers or between immiscible liquids. For interfacial profiles deviating from eq 7, the proportionality constant in eq 6 may be slightly different.

The observed intensity data for the angular range above $s = 0.097$ nm^{-1} (up to $s = 0.134$ nm^{-1} for the blends containing 3, 30, and 50% copolymer and up to $s = 0.175$ nm^{-1} for the blends containing 10, 20, and 40% copolymer) were fitted to eq 5 by means of a nonlinear least-squares program. Figure 9 plots the values of σ thus obtained

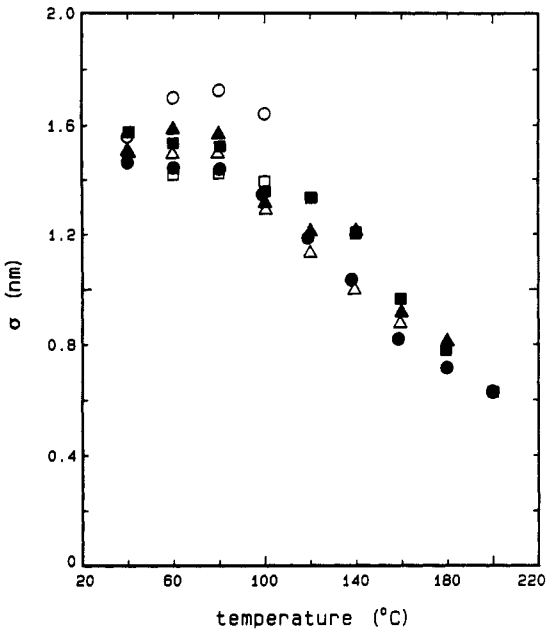

Figure 9. Interface thickness parameter, σ, obtained from Porod's law analysis of neutron scattering data on the basis of eq 5 plotted against the temperature of measurement: ϕ = (○) 49.0%; (●) 40%; (□) 29.8%; (■) 19.7%; (△) 10.1%; (▲) 3.0%.

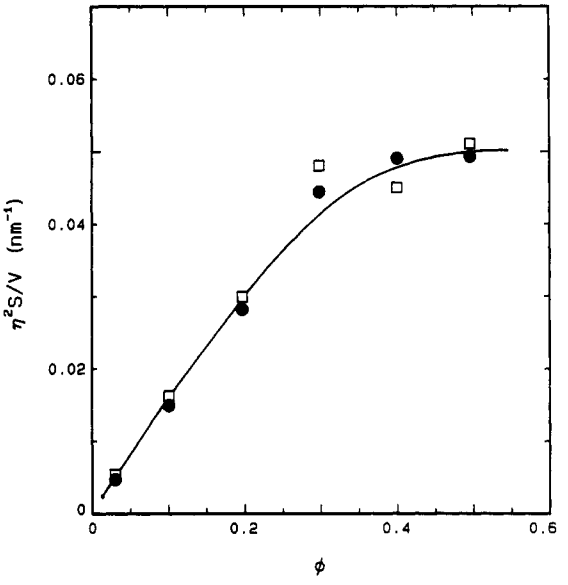

Figure 10. Product of S/V and η^2, evaluated from Porod's law analysis of neutron scattering data on the basis of eq 5 plotted against the volume fraction, ϕ, of copolymer in the sample. S/V is the specific interfacial area between the copolymer phase and deuteriated polybutadiene phase, and $1 - \eta$ is the degree of swelling of the copolymer phase by the deuteriated polybutadiene: circles, 60 °C; squares, 120 °C.

against the temperature. It shows, first of all, that the interfacial layer thickness remains unchanged when the concentration of copolymer in the system is increased. It also shows that the thickness decreases markedly as the temperature is increased, the implication of which is discussed in the next section. Figure 10 gives the value of η^2S/V against the volume fraction, ϕ, of copolymer in the system for two temperatures, 60 and 120 °C. At low copolymer concentration ($\phi \leq 0.3$), η^2S/V values are roughly proportional to ϕ, suggesting that the average dimension of the styrene microdomains remains about the same even as more copolymer is added and consequently more micelles or micellar aggregates are formed. Figure 11 plots the value of η^2S/V against temperature for the

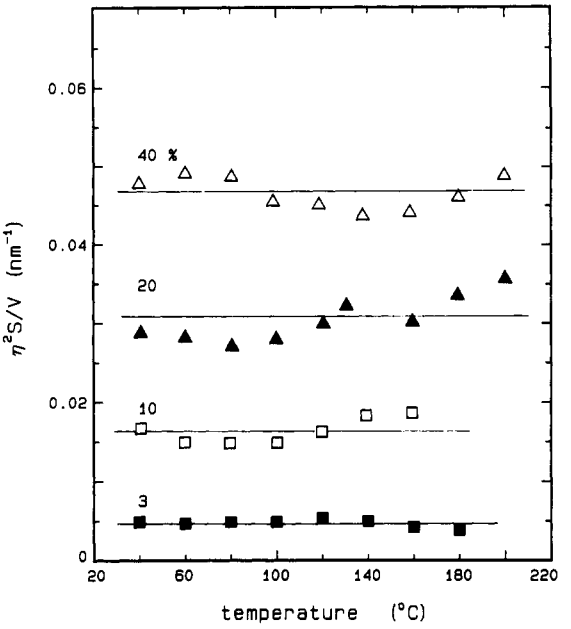

Figure 11. Product η^2S/V evaluated from Porod's law analysis of neutron scattering data plotted against temperature. The volume fraction, ϕ, of copolymer in the sample is indicated.

systems containing various concentrations of the copolymer. The constancy of η^2S/V over the temperature range studied arises from the contrary temperature dependences of η and of S. The value of η, which is the volume fraction of styrene in the styrene microdomain swollen with deuteriated polybutadiene, decreases at higher temperature, while the number of micelles or micellar aggregates increases with temperature, and the temperature dependences of these two quantities evidently balance out each other. For low concentrations of copolymer (ϕ = 0.03 and 0.10) both the X-ray and neutron scattering data can be analyzed in terms of spherical micelles to obtain more explicit results that essentially substantiate the qualitative features deduced above.

Although X-ray data could in principle be analyzed in terms of Porod's law as above, this was not pursued as the precision of the X-ray intensity data obtained at large s in Porod's region was not sufficient for such an analysis.

(iv) Micelle Structure. At low concentrations, 3 and 10%, the block copolymer molecules are very likely to be present as spherical micelles without any appreciable aggregation. The X-ray and neutron scattering intensity data at these two concentrations are therefore further analyzed by methods appropriate to systems consisting of suspensions of spherical particles.

It was previously shown that the Percus–Yevick solution[18-20] for the structure factor of hard-sphere liquids can serve as a model for calculating predicted scattering curves to fit observed data and thereby allow[7,21] evaluation of parameters characterizing the block copolymer micelles. The procedure for calculating predicted scattering curves and fitting to observed data was described in detail in our previous work.[7] The model assumes the following. The individual micelle consists of a spherical core of radius R. The polydispersity in R is represented by the Flory–Schultz distribution

$$W(R) = (1/z!)b^{z+1}R^z \exp(-bR) \quad (8)$$

where the parameter z characterizes the width of the distribution ($z = \infty$ corresponding to a δ function) and the parameter b is related to the number-average radius $\langle R \rangle$ by $b = (z + 1)/\langle R \rangle$. The micelle core is surrounded by a

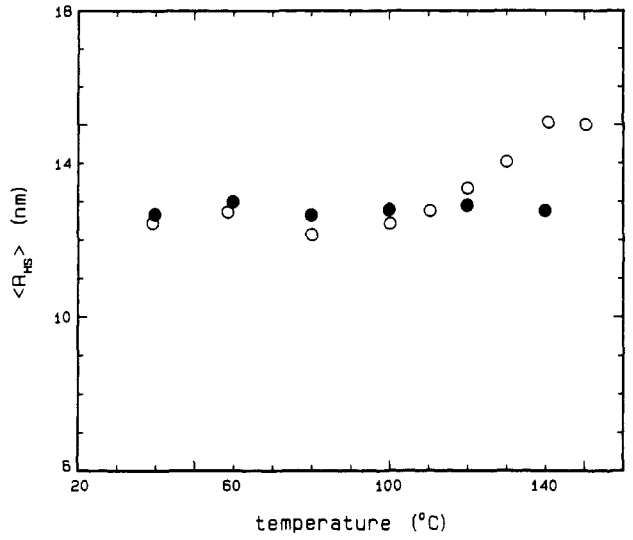

Figure 12. Effective hard-sphere radius R_{HS} of spherical micelles evaluated by fitting the Percus–Yevick hard-sphere liquid model to the scattered intensity curves obtained from the mixture containing 3% copolymer. $\langle R_{HS} \rangle$ denotes the number-average of R_{HS}. The solid symbols refer to results obtained from neutron scattering data and the open symbols from X-ray data.

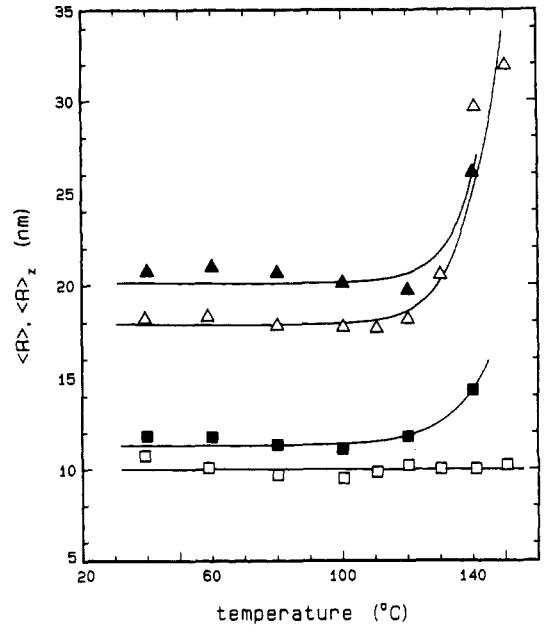

Figure 13. Effective core radius, R, of spherical micelles evaluated by fitting the Percus–Yevick hard-sphere liquid model to the scattered intensity curves obtained from the mixture containing 3% copolymer. The solid symbols refer to results obtained from neutron scattering data and the open symbols from X-ray data. Squares are number-average values, and triangles are z-average values.

shell (or corona) of butadiene blocks swollen with deuteriated polybutadiene, and therefore the distance of closest approach between two micelles is characterized by a "hard-sphere" radius R_{HS}, where $R_{HS} > R$. The micelle core of radius R in this model corresponds to the region at the micelle center where the scattering density is different from the polybutadiene matrix. Thus, for X-ray scattering the core is the central region occupied by styrene blocks, exclusive of butadiene blocks, while for neutron scattering the value of R is somewhat larger since the core now includes the protonated central region occupied by both butadiene and styrene blocks of the copolymer.

With use of the three parameters $\langle R \rangle$, $\langle R_{HS} \rangle$, and z as adjustable parameters, the calculated curve was fitted against the observed curve by minimizing the mean-square deviation between the two by means of a numerical algorithm based on the Gauss–Newton method. Figure 12 gives the values of $\langle R_{HS} \rangle$ thus evaluated for the sample containing 3% block copolymer. A good agreement between the $\langle R_{HS} \rangle$ values obtained from the two sets of data is seen. Figure 13 plots the number-average core radii, $\langle R \rangle$, obtained from the X-ray and neutron data, and the corresponding z-average values, $\langle R \rangle_z$, calculated by $\langle R \rangle_z = \langle R \rangle (z+8)^{1/2}(z+7)^{1/2}/(z+1)$. As the schematic diagram in Figure 14 shows, the "effective" core radius obtained from neutron data is larger than the "true" core radius from X-ray data, and furthermore both are smaller than $\langle R_{HS} \rangle$. The comparison of the number-average, $\langle R \rangle$, and z-average, $\langle R \rangle_z$, core radii given in Figure 13 shows that the polydispersity of the micelle size remains relatively unchanged up to about 120 °C and then increases rapidly as the temperature is raised until the micelles dissolve into the matrix. The values of $\langle R_{HS} \rangle$ and $\langle R \rangle$ obtained for the sample containing 10% copolymer are approximately the same as those shown in Figures 12 and 13 within the experimental error.

The adjustment of the three parameters $\langle R \rangle$, $\langle R_{HS} \rangle$, and z is sufficient to achieve fitting of the *shape* of the observed scattering curve by the calculated one. But to match the *absolute intensity* of the calculated curve to the observed one, an additional parameter needs to be adjusted, since the magnitude of the scattered intensity depends, in addition, on the number of micelles per unit volume and

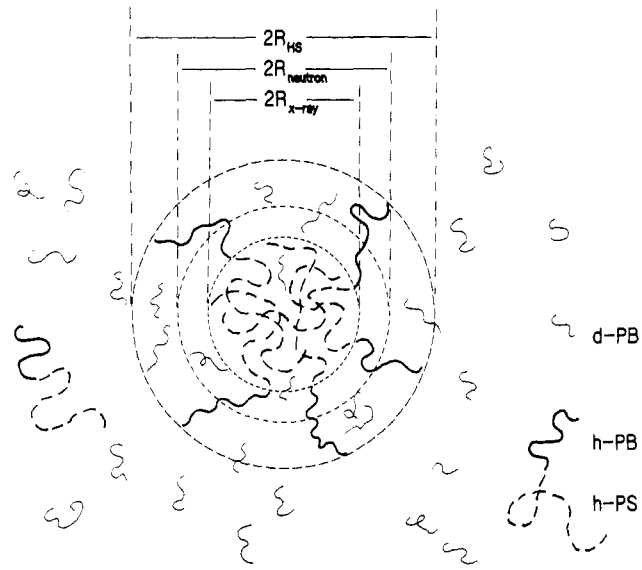

Figure 14. Schematic illustration of a spherical micelle. The hard-sphere radius, R_{HS}, the "effective" core radius, $R_{neutron}$, obtainable from neutron scattering data, and the "true" core radius, $R_{X\text{-}ray}$ obtainable from X-ray scattering data are indicated.

also on the scattering density contrast between the micelle core and the matrix. The latter depends on the degree of swelling of the micelle core by the deuteriated polybutadiene. The number density, N, of micelles and the volume fraction, η, of styrene units in the micelle core are related to each other through the following equation expressing the mass balance of copolymer in the system:

$$\phi' = N\langle V \rangle \eta + \phi_c'(1 - N\langle V \rangle \zeta^3) \qquad (9)$$

Here, $\langle V \rangle$ is equal to $(4/3)\pi\langle R^3 \rangle$, and ζ is the ratio R_{HS}/R. The symbols ϕ' and ϕ_c' are to be interpreted differently, according to the type of scattering being considered. For neutron scattering data, ϕ' and ϕ_c' denote the concentration (volume fraction) of copolymer in the mixture and the critical micelle concentration, respectively, while for X-ray

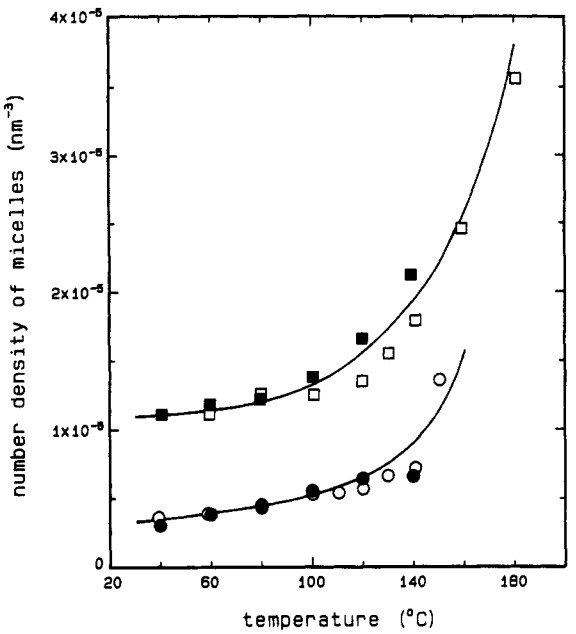

Figure 15. Number density, N, of micelles evaluated from a fit of the Percus–Yevick hard-sphere liquid model to the absolute intensity of scattering from mixtures containing 3 (circles) and 10% (squares) copolymer. The solid symbols refer to results obtained from neutron scattering data and the open symbols from X-ray scattering data.

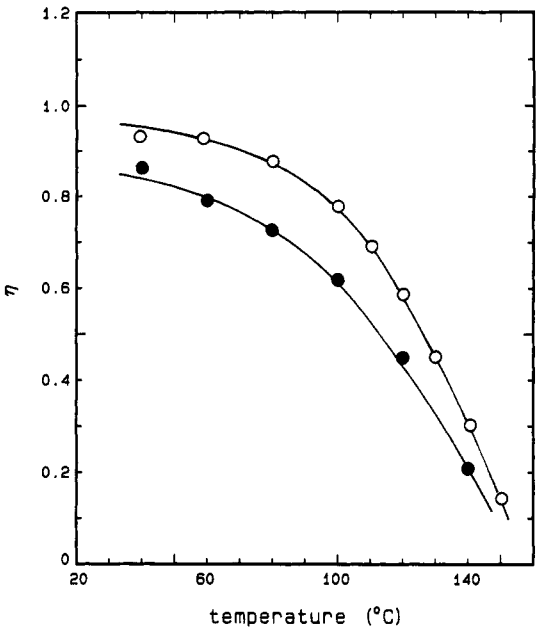

Figure 16. Value of η evaluated from a fit of the Percus–Yevick hard-sphere liquid model to the absolute intensity of scattering from the mixture containing 3% copolymer. The solid symbols refer to results obtained from neutron scattering data and the open symbols from X-ray scattering data. The value $1 - \eta$ in the case of X-ray data corresponds to the degree of swelling of the styrene core by polybutadiene, while the value $1 - \eta$ in the case of neutron data corresponds to the degree of swelling of the *effective* core that includes the inner part of the corona as well as the styrene core.

data, ϕ' and ϕ_c' refer to the corresponding volume fractions of *styrene units* only. In utilizing eq 9, we used the value of the critical micelle concentrations determined in the previous study[7] in which the same copolymer was added to a hydrogenated polybutadiene having a molecular weight very close to that of deuteriated polybutadiene used in this work. Any error in the value of ϕ_c' affects the relationship between N and η only insignificantly, since in eq 9 the second term involving ϕ_c' is much smaller than the first term.

By treatment of N (or η) as an adjustable parameter under the constraint of eq 9 and calculation of the intensity curve to match the absolute intensities of the observed data, the values of N and η were determined and are plotted in Figures 15 and 16. The agreement between the values of the micelle number densities, N, obtained from the neutron and X-ray data is very good. As the temperature is raised, the increase in the number density of micelles is accomplished without reducing the core radius, $\langle R \rangle$, of the micelles as a result of increased swelling of the styrene block by polybutadiene. The agreement in the values of η between X-ray and neutron results is less close, in part because of the fact that the meaning of η is somewhat different between X-ray and neutron cases. In the X-ray case, η signifies the volume fraction of styrene units in the micelle core and $1 - \eta$ thus gives the degree of swelling of the core by the deuteriated polybutadiene. In the neutron case, $1 - \eta$ signifies the degree of penetration of the deuteriated polybutadiene into the (hydrogenated) block copolymer phase, which includes both the micelle core and the corona. Since the polybutadiene is more readily miscible with the butadiene blocks in the corona, the η values deduced from neutron data are always lower than the values deduced from X-ray data.

Discussion

When due considerations are given to the difference in the origin of the contrast giving rise to the X-ray and neutron scatterings, the results derived from the two types of measurements presented above are entirely consistent with each other. The combination of the two techniques thus affords confirmation of the essential correctness of the conclusions drawn, in spite of the errors associated with individual data points.

The results presented in Figures 12–16 are based on the assumption that at low copolymer concentration—3% and possibly at 10%—the copolymer micelles are spherical. Electron microscopic observation[22] of a styrene–butadiene block copolymer added to a polystyrene matrix indeed shows that a spherical, as opposed to cylindrical, shape is favored when the copolymer concentration is low and the polystyrene molecular weight is low. At 3% concentration, the micelles are far apart from each other, so that the scattering intensity curve can be analyzed in terms of Guinier's law. The micelle radius determined in this way agrees fairly well with those determined by the Percus–Yevick fitting and presented in Figure 13, thus lending support to the assumption of spherical shape. As the copolymer concentration is increased, however, it is likely that the micelles transform into cylindrical and lamellar form and at the same time the degree of aggregation progressively increases. The continual decrease in the effective interdomain separation, d, with increasing concentration as seen in Figures 3–5 is consistent with such a picture. The data in Figure 5 show that the exponent a in the relationship $d \propto \phi^{-a}$ is substantially larger than $^1/_3$. This suggests that the mean distance between micelles (or microdomains) is reduced more rapidly than is dictated by the increase in the amount of copolymer alone. Thus, either the micelles are getting smaller with increasing ϕ with the shape of the micelles remaining unchanged or alternatively the shape of the micelles is altered with increasing ϕ. The first of the above is ruled out by the results in Figure 10 suggesting that, with η invariant with ϕ, an approximate proportionality of the specific interfacial area, S/V, to ϕ holds up to about $\phi = 0.3$. Some clues to the occurrence of morphological transformation of the mi-

celles could be obtained, in principle, if the scattering curves are carefully scrutinized. Such an analysis may, however, be difficult or inconclusive, when the system contains a mixture of micelles of different shapes and sizes and also when the boundary layer of the micelles is diffuse, as is expected in the present case. Electron microscopy, in conjunction with scattering studies, is likely to be more fruitful for this purpose.

Another important assumption employed throughout the analysis is that the material can be considered a two-phase system. In the case of X-ray scattering, the small difference (see Table I) in the electron density between hydrogenated and deuteriated polybutadienes can be neglected and the assumption is certainly valid. The neutron scattering length density difference between polystyrene and hydrogenated polybutadiene is small although it may not be negligible. The contrast between the styrene core and the butadiene corona depends, however, mostly on the concentration of deuteriated polybutadiene that has penetrated into the respective regions. The concentration is obviously much higher in the corona than in the core. Within the corona itself, the deuteriated polybutadiene is likely to be distributed nonuniformly, with a much higher concentration in the outer layer than near the core–corona interface. As a result, a gradient in scattering length density is set up within the corona, and as far as neutron scattering is concerned the virtual "interface" between the two phases may exist somewhere within the corona. The "interface" will be very broad, and its thickness may, in fact, extend from near the true corona–core interface to a point beyond R_{HS}. (The latter represents the separation at which interaction between micelles has become repulsive, and this will arise only after some interpenetration of copolymer blocks in neighboring micelles has already occurred.) At low temperatures, the interfacial thickness parameter, t, evaluated by eq 6 amounts to about 3.5 nm, and this is indeed larger than the difference of 2.0 ± 0.5 nm between R_{HS} and R_{core} (see Figures 12–14). The interfacial thickness may also be compared with the rms end-to-end distance of the hydrogenated butadiene block of the copolymer, which should be 6.3 ± 0.6 nm, assuming a characteristic ratio in the range 4–6. This is much larger than the difference between R_{HS} and R_{core}, again suggesting that repulsion between two micelles develops only at a sufficiently close distance where the highly swollen coronas belonging to the two micelles overlap with each other to a significant extent.

At higher temperatures, above 100 °C, both neutron and X-ray data indicate a decrease in the interfacial thickness parameter. This is accompanied by an apparent increase in the amount of butadiene homopolymer in both the micelle core and corona, with little change in the core size. Within the context of the two-phase model, these findings can be rationalized by noting that the dominant feature involves an increased penetration of the homopolymer within the micelle corona and a smaller and uniform penetration into the core. The interface thickness obtained by neutron scattering at low temperature is large because the concentration gradient of the penetrated deuteriated polybutadiene in the corona is very shallow. In contrast, the gradient becomes steeper at higher temperatures as the deuteriated polybutadiene penetrates deeper until it encounters a barrier presented by the corona–core boundary. This explains the reduction in the apparent interfacial thickness obtained by neutron scattering at higher temperature, as shown in Figure 9.

Acknowledgment is made to the donors of the Petroleum Research Fund, administered by the American Chemical Society, for the support of this research.

References and Notes

(1) Meier, D. J. In *Thermoplastic Elastomers*; Legge, N. R., Holden, G., Schroeder, H. E., Eds.; Hanser Publishers: New York, 1987; p 269.
(2) Hashimoto, T. In *Thermoplastic Elastomers*; Legge, N. R., Holden, G., Schroeder, H. E., Eds.; Hanser Publishers: New York, 1987; p 349.
(3) Roe, R. J.; Rigby, D. *Adv. Polym. Sci.* **1987**, *82*, 103.
(4) Roe, R. J.; Zin, W. C. *Macromolecules* **1984**, *17*, 189.
(5) Zin, W. C.; Roe, R. J. *Macromolecules* **1984**, *17*, 183.
(6) Rigby, D.; Roe, R. J. *Macromolecules* **1984**, *17*, 1778.
(7) Rigby, D.; Roe, R. J. *Macromolecules* **1986**, *19*, 721.
(8) Nojima, S.; Roe, R. J. *Macromolecules* **1987**, *20*, 1866.
(9) Disclaimer: Certain commercial materials and equipment are identified in this paper in order to specify adequately the experimental procedure. In no case does such identification imply recommendation or endorsement by the National Institute of Standards and Technology nor does it imply necessarily the best available for the purpose.
(10) Strobl, G. R. *Acta Crystallogr.* **1970**, *A26*, 367.
(11) Glinka, C. J.; Rowe, J. M.; LaRock, J. G. *J. Appl. Crystallogr.* **1986**, *19*, 427.
(12) Richardson, M. J.; Savill, N. G. *Polymer* **1977**, *18*, 3.
(13) Brandrup, J., Immergut, E. H., Eds. *Polymer Handbook*, 2nd ed.; Wiley: New York, 1975; Section V.
(14) Bates, F. S.; Dierker, S. B.; Wignall, G. D. *Macromolecules* **1986**, *19*, 1938.
(15) Porod, G. *Kolloid-Z.* **1951**, *124*, 83.
(16) Ruland, W. *J. Appl. Crystallogr.* **1971**, *4*, 70.
(17) Roe, R. J.; Fishkis, M.; Chang, J. C. *Macromolecules* **1981**, *14*, 1091.
(18) Percus, J. K.; Yevick, G. J. *Phys. Rev.* **1958**, *110*, 1.
(19) Vrij, A. *J. Chem. Phys.* **1979**, *71*, 3267. Van Beurten, P.; Vrij, A. *J. Chem. Phys.* **1981**, *74*, 2744.
(20) Kotlarchyk, M.; Chen, S. H. *J. Chem. Phys.* **1983**, *79*, 2461.
(21) Kinning, D. J.; Thomas, E. L. *Macromolecules* **1984**, *17*, 1712.
(22) Kinning, D. J.; Winey, K. I.; Thomas, E. L. *Macromolecules* **1988**, *21*, 3502.

Registry No. (Styrene)(butadiene) (block copolymer), 106107-54-4.